

# Structural, Spectroscopic and Dielectric Study of CuS Nanoparticles

N. S. Tank<sup>1</sup>, K. D. Parikh<sup>2\*</sup>, B. V. Jogiya<sup>3\*</sup> and M. J. Joshi<sup>1</sup>

<sup>1</sup>Department of Physics, Saurashtra University, Rajkot, 360005, India.

<sup>2</sup>Department of Physics, Gujarat Arts and Science College, Ahmedabad, 380,006, India.

<sup>3</sup>Regional Forensic Science Laboratory, Rajkot, 360,005, India.

\*Corresponding author: ketandparikh@yahoo.co.in and bhoomika.cpi@gmail.com

## Abstract

CuS nanoparticles are successfully synthesized via the co-precipitation method. The powder XRD confirmed the hexagonal structure. The average particle size of CuS nanoparticles were calculated by the Scherrer's formula and found to be 2.71 nm. TEM image indicated spherical shape with average particle size is 6.89 nm. The FTIR spectral study confirmed the presence of S-O stretching, O-H bending, and S-S disulphide stretching vibrations. The EDAX analysis is done confirm the presence Cu and S in present nanoparticles. The dielectric constant versus frequency plot exhibited characteristic nature with decreasing value of dielectric constant with increase in frequency.

**Keywords:** CuS nanoparticles, powder XRD, FT-IR, EDAX and Dielectric study.

Date of Submission: 23-05-2022

Date of Acceptance: 05-06-2022

## I. Introduction

Copper Sulphide (CuS) nanomaterials are widely used for different applications, such as p-type semiconductors in solar cells [1-3], as optical filters [4], as a super ionic material [5], the photo catalytic activity of CuS nano-flowers [6], photo-voltaic applications [7] and microwave shielding coatings [8]. Moreover, copper sulphide nanoparticles are used for combined photo acoustic imaging, tumour-selective chemotherapy and photo thermal therapy as a enzyme-responsive particles [9]. Special attention is given to the study of copper sulphide thin films due to the discovery of the CdS/Cu<sub>2</sub>S hetero junction solar cell [10]. CuS finds application in photo thermal therapy [11], to apply local heating to kill cells. In search of new semiconducting materials for efficient solar energy conversion and photo electrochemical solar cells, metal oxides and chalcogenides are studied [12]. Sulphide-based luminescent materials have attracted a lot of attention for a wide range of photo-cathode and electroluminescent applications. Recently, sulphide materials have regained interest due to their ability (in contrast to oxide materials) to provide a broad band, Eu<sup>+2</sup> based red emission for use as a color conversion material in white-light emitting diodes (LEDs). The potential application of rare-earth doped binary alkaline-earth sulphides, like CaS and SrS, along with other sulphides are reviewed [13]. Among various nanomaterials, II-VI class inorganic semiconductor nanomaterials like CuS are proved to be versatile materials. The main advantage of these semiconductors is that, they are made up of a group of direct wide band gap semiconductors, which is very important for photovoltaic applications. These semiconducting nanomaterials, because of their wide direct band gap, are desired for the next generation optoelectronic communication systems, optical recording devices, light sensors and blue diode lasers.

## II. Experimental

In the present study, aqueous chemical method was employed for synthesis of copper sulphide (CuS) nanoparticles. Analytical grade CuCl<sub>2</sub> and Na<sub>2</sub>S was selected as starting materials and used them without any further purification. Both the precursor materials were water soluble therefore, double distilled water was selected as a solvent. The chemical reaction scheme is given below.



1M CuCl<sub>2</sub> was dissolved in 100ml distilled water and the solution 1M sodium sulphide (Na<sub>2</sub>S) was added in a drop wise manner under constant stirring using a magnetic stirrer at 70°C, which resulted in to formation of CuS nano-collide. The nano particles were collected on filtration using Whatman filter paper of number 1 and further washed by distilled water. The samples were dried using microwave oven for 3 hours at 85°C. The dried samples were used for further characterizations.

### III. Result And Discussion

#### Powder X-ray Diffraction Study:

Powder diffraction is a scientific technique using X-ray diffraction on powder or micro crystalline samples for structural characterization of materials[14]. In this technique material is used in powder form as every possible crystalline orientation is represented nearly equal in a powdered sample. The term 'powder' really means that the crystalline domains are randomly oriented in the sample. Therefore, when the 2-D diffraction pattern is recorded, it shows concentric rings of scattering peaks corresponding to the various d spacing in the crystal lattice. The positions and the intensities of the peaks are used for identifying the underlying structure (or phase) of the material.

The method has been traditionally used for phase identification, quantitative analysis and the determination of structure imperfections. Nowadays applications have been extended to new areas, such as the determination of crystal structures and the extraction of three-dimensional micro-structural properties. Powder diffraction data are usually presented as a diffractogram in which the diffracted intensity  $I$  is shown as a function of the scattering angle  $2\theta$ . Relative to other methods of analysis, powder diffraction allows for rapid, non-destructive analysis of multi-component mixtures without the need for extensive sample preparation[15].

The most widespread use of powder diffraction is in the identification and characterization of crystalline solids, each of which produces a distinctive diffraction pattern. In contrast to a crystalline pattern consisting of a series of sharp peaks, amorphous materials (liquids, glasses etc.) produce a broad background signal. XRD can be used to determine the crystallinity by comparing the integrated intensity of the background pattern to that of the sharp peaks. The diffraction lines of a powder XRD pattern will be very sharp for a crystalline material consisting of sufficiently large and strain-free crystallites[15], therefore, the powder XRD line broadening (peak width) inversely correlates the crystallite size and lattice perfection.

From the measurement of diffracted peak positions in XRD one can characterize homogeneous and inhomogeneous strains. Homogeneous or uniform elastic strain shifts the diffraction peak positions. From the shift in peak positions, one can calculate the change in d-spacing, which is the result of the change of lattice constants under a strain. In homogeneous strains vary from crystallite to crystallite or within a crystallite and this causes a broadening of the diffraction peaks that increase with  $\sin\theta$ . Peak broadening is also caused by the finite size of crystallites; however, in this case, the broadening is independent of  $\sin\theta$ . When both crystallite size and inhomogeneous strain contribute to the peak width, these can be separately determined by careful analysis of peak shapes.

If there is no inhomogeneous strain, the crystallite size can be estimated from the peak width with the Scherrer's formula. However, one should be alerted to the fact that nanoparticles often form twinned structures; therefore, Scherrer's formula may produce results different from the true particle sizes. In addition, X-ray diffraction only provides the collective information of the particle sizes and usually requires a sizable amount of powder. It should be noted that since the estimation would work only for very small particles. The significant broadening of the XRD pattern peaks reveals the smaller size of the particles. The similar results are reported by Tank et al. [16].

In the present investigation CuS nanoparticles were analyzed by PHILIPSPMD with Cu-K $\alpha$  radiation. The crystal structure was determined by computer software Powder- X. The estimated values of unit cell dimensions are given in Table 1.

**Table 1:** Unit cell parameters of CuS nanoparticles.

Sample	a(Å)	b(Å)	c(Å)	Structure
CuS	3.757	3.757	16.19	Hexagonal

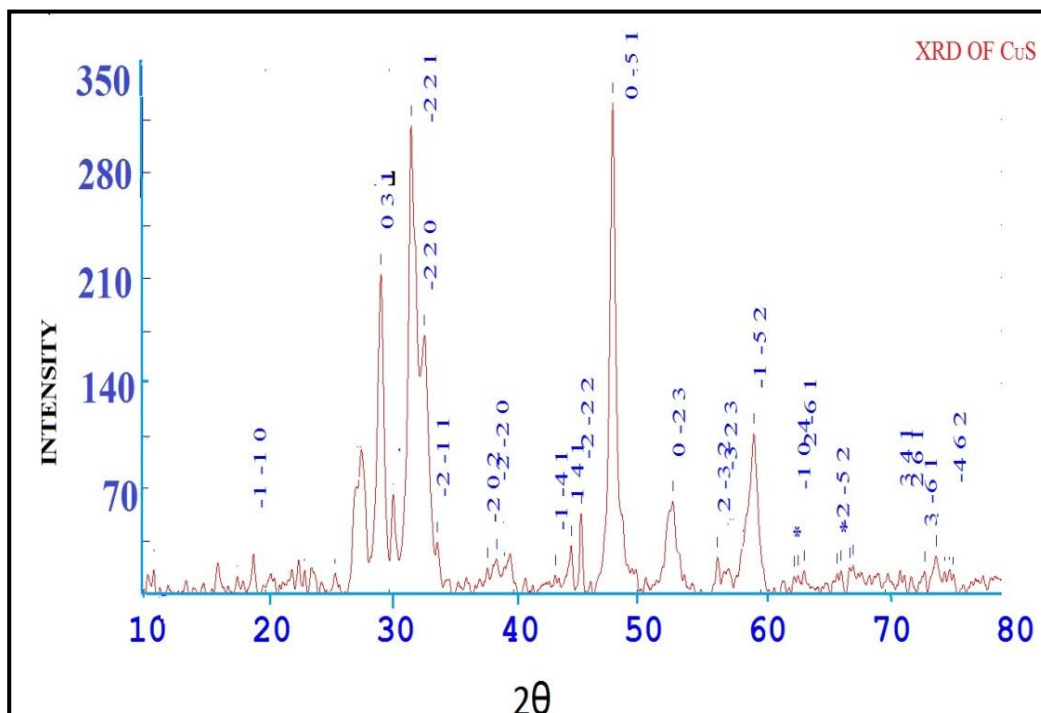


Figure 1: XRD spectra for CuS nanoparticles.

Figure 1 exhibits the powder XRD pattern of pure CuS nanocrystals. All major reflections in the XRD pattern were fitted and assigned to the corresponding plane. Pure CuS nanoparticles are found to have hexagonal crystal structure [17].

**Scherrer's Formula:**

In the present investigation the average particle size of CuS nanoparticles are calculated by the Scherrer's formula [19], which is as follows:

$$D = \frac{k\lambda}{\beta \cos\theta} \dots \dots \dots (1)$$

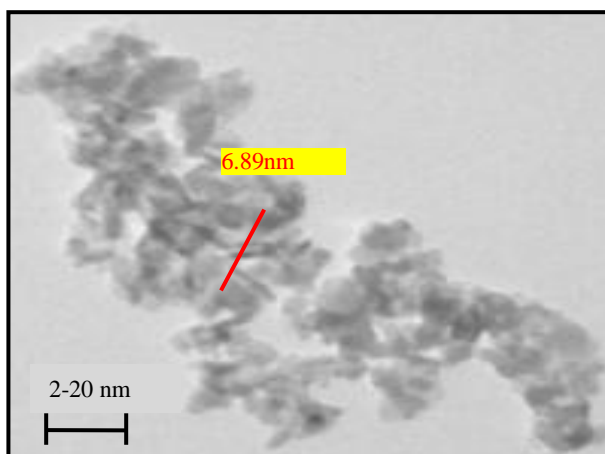
Where,  $\lambda$  = Wave length of Source = 1.54178 Å for Cu K $\alpha$ , D = Average crystallite size,  $\beta$  is the full width at half maximum (FWHM) of that peak in radian.

From this formula the average particle size of CuS nanoparticles were calculated and found to be 2.71nm. Earlier, Gautam and Mukherjee [18] reported the nanoparticles of 11nm calculated by powder XRD.

**Transmission electron microscopy studies:**

Figure 2: TEM image for CuS nanoparticles.

The Transmission Electron Microscopy (TEM) and the High-Resolution Transmission Electron Microscopy



(HR-TEM) are the popular techniques for characterization of nanoparticles. TEM images give an immediate

visualization of the particles which provides direction formation of the size, shape, dispersion, structure and morphology of nano-systems. TEM images usually complement to XRD data and also enable to observe details at a nanometer scale. However, it should be noted that this technique gives image of a very small section of the material. In the present study TEM analysis was carried out on Philips Technai-20. The material was dispersed in acetone and put on grid. Figure 2 depict the TEM image for CuS nanoparticles. It can be observed from figure 2 that CuS nanoparticles are large often agglomerated. The agglomeration may be occurring due to reduce the surface energy by weakly connecting through the dangling bonds on the surface. All the nanoparticles have nearly spherical morphology. The observed particle size is 6.89nm[19], which is slightly higher than the average particle size obtained from the Scherrer's formula. This due to considering only one particular nanoparticle and not all particles observed in the image.

**FT-IR spectroscopy studies:**

FT- IR is a convenient technique to rapidly identify the presence of certain functional groups present in a structure. Infrared spectroscopy reveals information about molecular vibrations that cause a change in the dipole moment of molecules. It offers a fingerprint of the chemical bonds present within materials. When radiation passes through a sample (solid, liquid or gas) certain frequencies of the radiation are absorbed by the molecules of the substance leading to the molecular vibrations. The frequencies of absorbed radiation are unique for each molecule which provides the characteristics of a substance. In present study FTIR spectrum of CuS nanoparticle were recorded on FT-IR spectrometer in Nicolet 6700FT-IR spectrometer. The spectrum in the range 400- 4000  $\text{cm}^{-1}$  is showing IR absorption due to the various vibrations involved.

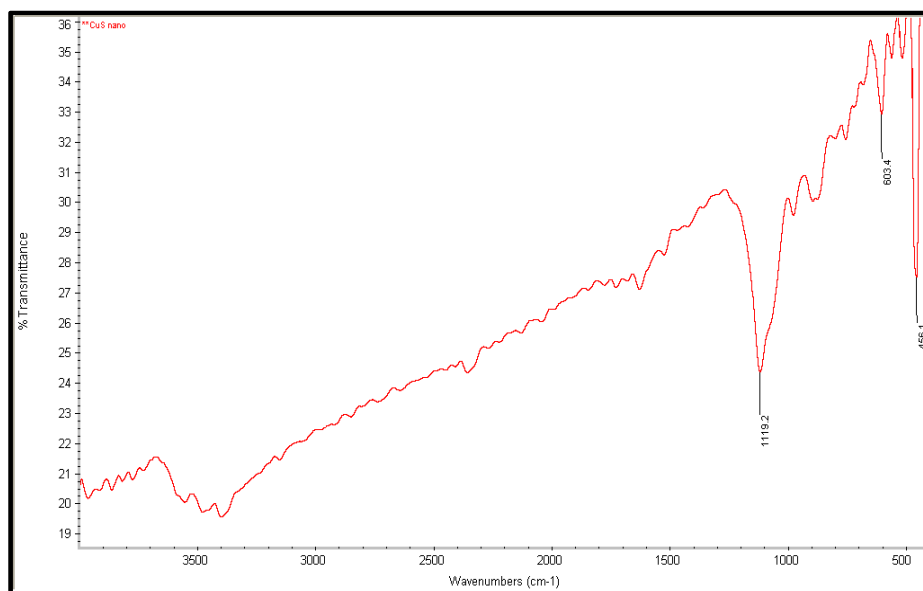


**Figure 3:** FT-IR spectra for CuS nanoparticles.

Figure 3 shows the FTIR spectrum of pure CuS nanoparticles. For pure CuS the major absorption at 1119.2  $\text{cm}^{-1}$  is due to asymmetric S-O stretching of the sulfate species and 600  $\text{cm}^{-1}$  and 456  $\text{cm}^{-1}$  are due to consequence of the disulfides stretch (S-S). The broad absorption at 3400  $\text{cm}^{-1}$  is due to moisture or adsorbed water. The broad and weak absorption around 900  $\text{cm}^{-1}$  indicates out of plane O-H bending [20]

**EDAX analysis:**

The composition analysis of the CuS nanoparticles was carried out by EDAX spectroscopy. The figure 4 is the EDAX plot for the synthesized CuS nano material and table 2 gives the values of weight percent and atomic weight percent for copper and sulphur, which confirms the presence of Cu and S.

From EDAX it is found that 74.67 wt.% corresponds to Cu and 25.33wt.% is corresponding to The molecular weight of CuS is 97.39 (with atomic weight of copper= 65.32 and sulphur=32.07). The atomic weight percent of copper is 67.07 and sulphur is 32.92 in ideal CuS. The ratio of Cu to S in CuS is equal to 2.03 in ideal CuS. In the present study the ratio of Cu to S is 2.94, considering even the percentage of errors in taking data (given in the table) the sample shows rich content of copper and sulphur deficit. The proposed formula can be obtained as CuS.

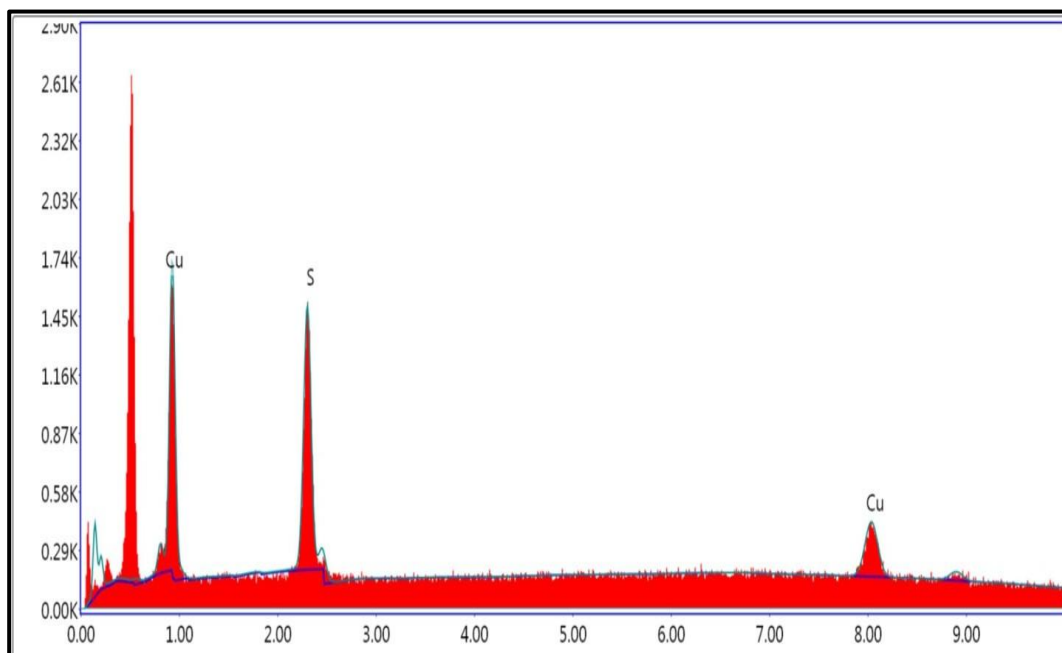


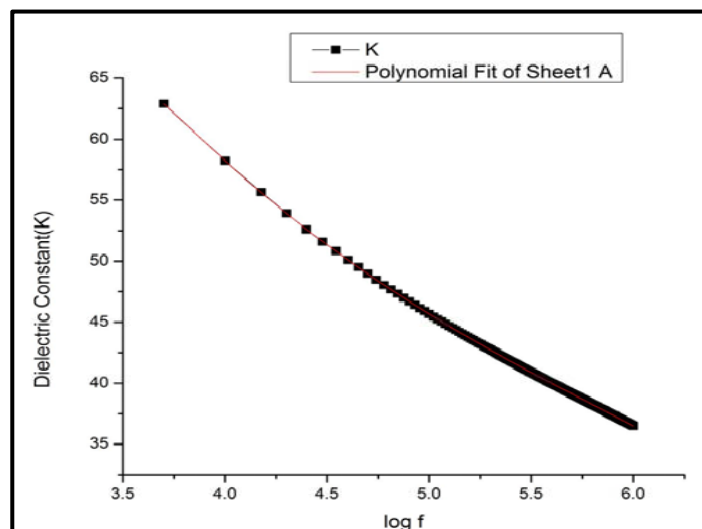
Figure 4: EDAX spectra of CuS nanoparticles.

Table 2: The values of weight percent and atomic weight percent for copper and Sulphur

Element	Weight %	Atomic %	Net Int.	Error %
S K	25.33	40.20	412.58	5.13
CuK	74.67	59.80	144.64	10.84

**Dielectric Study:**

The dielectric studies of copper sulphide thin films are reported in the frequency range from 50 Hz to 5 MHz by Saga devan and Murugesan [21]. The dielectric properties of nano-rods of copper sulphide is reported by Freeda et al [22]. In the present investigation, the values of dielectric constant were calculated from the measured values of capacitance at room temperature with in frequency range from 500Hz to 1MHz. Generally, the dielectric constant results due to the contributions of electronic, ionic and dipole orientation contributions to the polarisability. The variation of dielectric constant with frequency is displayed in figure 5 for CuS. From this plot one can observe that as the frequency increases the dielectric constant initially decreases very rapidly. This type of variation suggests that the higher space charge polarizability at lower frequency region. The electronic exchange of the number of ions in the crystal gives local displacement of electrons in the direction of applied field, which gives the polarization. As the frequency increases, a point is reached where the space charge cannot sustain and comply with the external field [21]. Therefore, the polarization decreases and exhibits the reduction in the values of dielectric constant as the frequency increases.



**Figure 5:** Plot of dielectric constant (K) versus log f

The variation in the dielectric loss ( $\tan \delta$ ) with frequency is shown in figure 6. This shows rapid decrease in loss value initially and then drops for the minimum as the frequency increases.

The nature of variation of a. c. conductivity ( $\sigma_{ac}$ ) is shown in figure 7. The frequency dependence of conductivity is a sum of d.c conductivity due to movements of free charges and polarization conductivity due to movements of bound charges. It is observed from the figure that the a.c conductivity increases gradually as frequency increases.

The electrical conductivity of copper sulphide was explained in detail on the basis of the structure by Vajenine and Hoffmann[23]. The compounds of the general formula  $MCu_{2n}X_{n+1}$ , where M is a mono-valent metal and X is a halogen, exhibit relatively high conductivity and an interesting structural pattern of copper-halogen layers. The electronic structure of a series of copper-sulfur layers with the  $Cu_{2n}S_{n+1}$  stoichiometry was studied using the extended Hückel method. Attention was focused on the unoccupied states at the top of the valence band. The states are Cu-S and Cu-Cu anti-bonding, which accounts for the observed contraction in the plane of the layers. The same states turn out to be strongly delocalized in the plane of the layers, with both copper and sulfur contribution; high mobility of holes in these states is responsible for the substantial conductivity observed in the corresponding materials. The idea of mesomeric reactions, borrowed from computational organic chemistry, was developed to address the relative stabilities of the copper-sulfur layers.

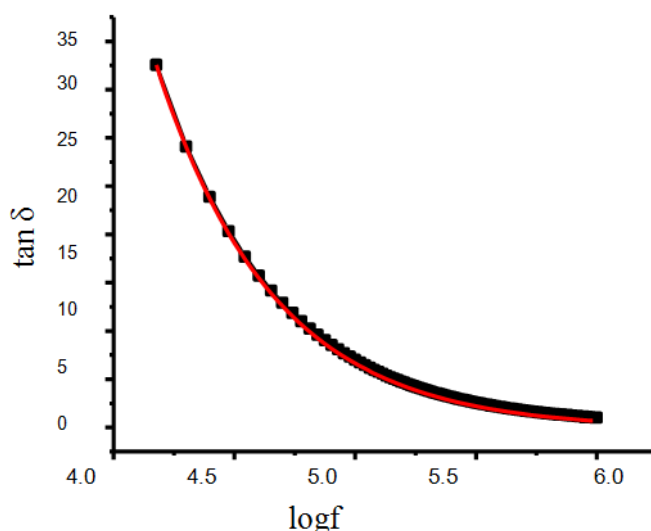


**Figure 6:** Plot of  $\tan \delta$  versus log f

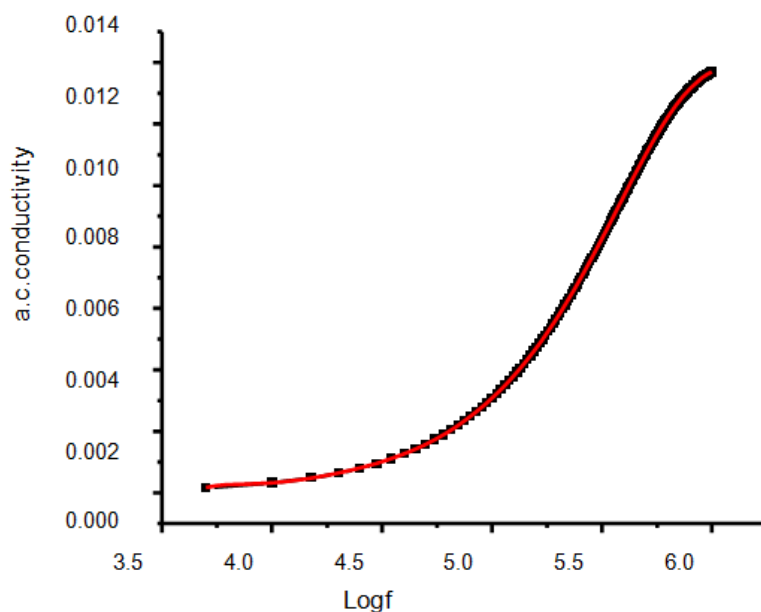


Figure 7: A.C. conductivity versus log f

Electrical conductivity measurements have been made on copper sulfide crystals of compositions ranging from  $\text{Cu}_{1.8}\text{S}$  to  $\text{Cu}_{2.0}\text{S}$  and indium-doped  $\text{Cu}_{1.8}\text{S}$  in the temperature region between  $20^\circ\text{C}$  and  $220^\circ\text{C}$  by Okamoto and Kawai[24]. Conductivity of  $\text{Cu}_{2-x}\text{S}$  varied from  $0.07\text{ohm}^{-1}\text{cm}^{-1}$  to  $2400\text{ohm}^{-1}\text{cm}^{-1}$  as the deviation from stoichiometry increased from  $x=0$  to  $x=0.2$ . It was found that  $\text{Cu}_{1.8}\text{S}$  (digenite) and  $\text{Cu}_{1.96}\text{S}$  (djurleite) undergo phase transitions at  $90^\circ\text{C}$  and at  $93^\circ\text{C}$  respectively. The transition temperature of  $\text{Cu}_2\text{S}$  (chalcocite) increased from  $98^\circ\text{C}$  to  $108^\circ\text{C}$  as conductivity decreased from  $52\text{ohm}^{-1}\text{cm}^{-1}$  to  $0.07\text{ohm}^{-1}\text{cm}^{-1}$ . An analysis of mixed conduction at  $\beta$  phase of low conductivity copper sulphide had shown that ionic conductivity was independent of the composition or the number of impurity cations in this material, and exhibited temperature dependence with activation energy of  $0.24\text{eV}$ .

#### IV. Conclusion

Copper sulphide nanoparticles were synthesized by using wet chemical co-precipitation method. The nanomaterial was synthesized without any capping agent, through eco-friendly path. The powder XRD study indicated hexagonal crystalline nature with unit cell parameter values  $a = b = 3.625\text{ \AA}$ ,  $c = 15.569\text{ \AA}$  and  $\alpha = \beta = 90^\circ$ ,  $\gamma = 120^\circ$ . The TEM study confirmed the nano-structured nature of the particles. Nearly spherical nanoparticles were found with  $6.89\text{ nm}$  size of a selected particle within the particles having range from  $2\text{ nm}$  to  $20\text{ nm}$ . The agglomeration of nanoparticles was also observed. The FTIR spectral study confirmed the presence of S-O stretching, O-H bending, and S-S disulphide stretching vibrations. EDAX analysis the stoichiometric formula of copper sulphide was obtained as  $\text{CuS}$ , indicating copper rich nanoparticles. The observed values of dielectric constant in response to frequency of applied field revealed that  $\text{Cu}_{1.28}\text{S}$  exhibited higher space charge polarizability at lower frequency region. The dielectric constant versus frequency plot exhibited characteristic nature with decreasing value of dielectric constant with increase in frequency.

#### References:

- [1]. Q. Xu, B. Huang, Y. Zhao, Y. Yan, R. Noufi and S. Wei, *Appl. Phys. Lett.*, **5**(2012)100.
- [2]. L. Isac, A. Duta, A. Kriza, S. Manolache and M. Nanu, *Thin Solid Films*, **9**(2007)515.
- [3]. T. Y. Ding, M. S. Wang, S. P. Guo, G. C. Guo and J. S. Huang, *Synth. Met.*, **2**(2011).
- [4]. H. Toyoji and H. Yao, *Jpn. Kokai Tokyo Koho JP02173,622*.
- [5]. A. Korzhuev, F. Khim, *Obrab. Mater.*, **3**(1993)131.
- [6]. T. Y. Ding, M. S. Wang, S. P. Guo, G. C. Guo and J. S. Huang, *Materials Letters*, **62**(2008)4529.
- [7]. W. Yue, W. Cyrus, M. Wanli, S. Bryce and A. Alivisatos, *Nano Letters*, **8**(2008)2551.
- [8]. M. Ramya and S. Ganesan, *Iranian J. of Sci & Tech.*, **37A3**(2013)293.
- [9]. Z. Zha, S. Zhang, Z. Deng, L. Yanyan, L. Changhui and D. Zhifei, *Chem. Commun.*, **49**(2013)3455.
- [10]. S. K. Haram, A. R. Mahadeshwar and S. G. Dixit, *J. of Phy. Chem.*, **100**(2014).
- [11]. J. Jiang, *Ann J Materials Sci Eng.*, **1**(2014)2.
- [12]. B. Subramanian, T. Mahalingam, T. Sanjeeviraja, M. aychandran and M. Chockalingam, *J. Of Material Science*, **16**(1999)357.
- [13]. F. S. Philippe, M. Iwan, H. Zeger and D. Poelman, *Materials*, **3**(2010)2834.
- [14]. B. D. Cullity, *Elements of X-ray Diffraction*, Addison Wesley Mass, ISBN 0-201-01174-3, chapter 14(1978).
- [15]. H. P. Klug and L. E. Alexander, *X-ray Diffraction Procedures for Polycrystalline and Amorphous Materials*, John Wiley and Sons,

- New York, **5**(1974)85.
- [16]. N. S. Tank, K. D. Parikh and M. J. Joshi, *AIP Conferences Proceedings* (2017) 1837.
- [17]. G. Cao, *Nanostructures and Nanomaterials*, Imperial College Press, London (2004).
- [18]. U. Gautam and B. Mukherji, *Bull. Mater. Sci.*, **29** (2006) 15.
- [19]. S. U. Offiah, P. E. Ugwoke, A. B. Ekwealor, S. C. Ezugwu, R. U. Osuji, F. I. Ezema, *Digest J. of Nanomaterials and Biostructures*, **1** (2012) 165.
- [20]. N. S. Tank, K. R. Rathod, K. D. Parikh and M. J. Joshi, *AIP Conferences Proceedings* (2016) 1728.
- [21]. S. Sagadevan and P. Murugasen, *Int. J. of Physical Sci.*, **8(21)**(2013) 1121.
- [22]. M. Annie Freedaa, C. K. Mahadevana, S. Ramalingom, *Archives of Physics Research*, **2(3)**, 2011, 175.
- [23]. Vajenine and Hoffmann, *Inorg. Chem.* **35**(1996), 451.
- [24]. K. Okamoto and S. Kawai, *Jpn. J. Appl. Phys.* **12** (1973) 1130.

N. S. Tank, et. al. "Structural, Spectroscopic and Dielectric Study of CuSNanoparticles." *IOSR Journal of Applied Chemistry (IOSR-JAC)*, 15(06), (2022): pp 01-08.